

Acceleration of picked-up interstellar helium ions at the Earth's bow shock: GEOTAIL observation

M. Oka¹, T. Terasawa¹, H. Noda¹, T. Mukai², and Y. Saito²

¹Department of Earth and Planetary Physics, University of Tokyo, Tokyo 113-0033, Japan

²Institute of Space and Astronautical Science, Sagami-hara 229, Japan

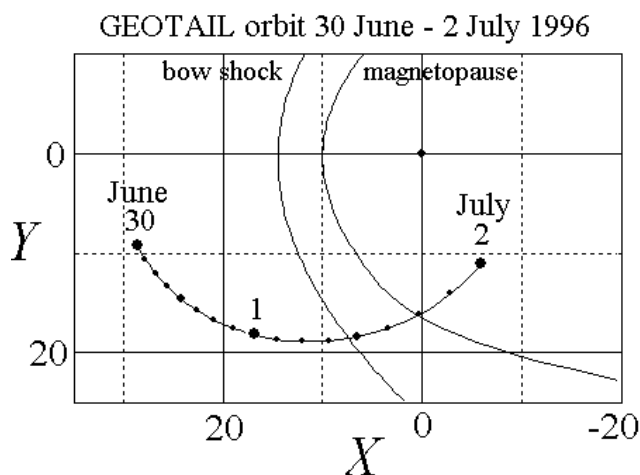


Fig. 1. The GEOTAIL orbit from 0 UT on 30 June 1996 to 0 UT on 2 July 1996. Nominal shapes of the bow shock and magnetopause are also drawn. The GEOTAIL crossing of the bow shock was in the dusk side of the bow shock at $(X, Y, Z)_{GSE} = (8.2, 18.5, -0.4) R_E$.

Abstract. After ionization in the solar wind, He^+ ions of the interstellar origin are expected to be accelerated at heliospheric shocks (the terminating shock, CIR shocks, and planetary bow shocks), and to become the seed population for anomalous cosmic rays. Although there are many theoretical attempts to treat the ‘injection’ process of these picked-up helium ions at these shocks, there have been few direct observational evidence. In this report we present the results of the case study of an event in which picked-up He^+ ions were reflected and accelerated at the earth’s bow shock.

1 Introduction

The pickup ions of interstellar origin have attracted considerable interests as a source of the accelerated particles produced at CIR shocks, the termination shocks, and planetary bow shocks. There are some observational evidence of the pickup ion acceleration at CIR shocks (e.g., Fraiz et al., 1999; Mason et al., 1999). It has been shown that pickup ion spectrum is hard and that lighter ions are more effectively accelerated compared to heavier ions (Gloeckler et al., 1994). At the termination shock, it is also expected that pickup ions are more efficiently accelerated than the thermal solar wind plasmas (e.g. Liewer et al., 1993; Gloeckler et al., 1994) and they are thought to be the source of the Anomalous Cosmic Rays (ACRs).

The mechanism of the initial acceleration of pickup ions has been mainly investigated through theoretical stand points (e.g., Giacalone and Jokipii, 1995; Zank et al., 1996; Lee et al., 1996; Lipatov and Zank, 1999; Ellison, 1999; Scholer and Kucharek, 1999). On the other hand, Mobius et al. (1985) first reported the detection of pickup He^+ of the interstellar origin from the earth-orbiting AMPTE satellite. It is, therefore, expected that some of the He^+ picked-up in the earth’s neighborhood will come to interact with the bow shock and get accelerated there. In this paper we report the first identification of the initial acceleration process of pickup He^+ at the bow shock.

2 Observation and Simulation

We utilize datasets of ions from LEP/EAI and LEP/SWI experiments on GEOTAIL (Mukai et al., 1994), as well as magnetic field data from MGF experiment (Kokubun et al., 1994). Our observation is the inbound crossing of dusk side of the bow shock around 10:47-10:48 on 1 July 1996. The position of the spacecraft is shown in the Figure 1.

Correspondence to: T. Terasawa
(terasawa@eps.s.u-tokyo.ac.jp)

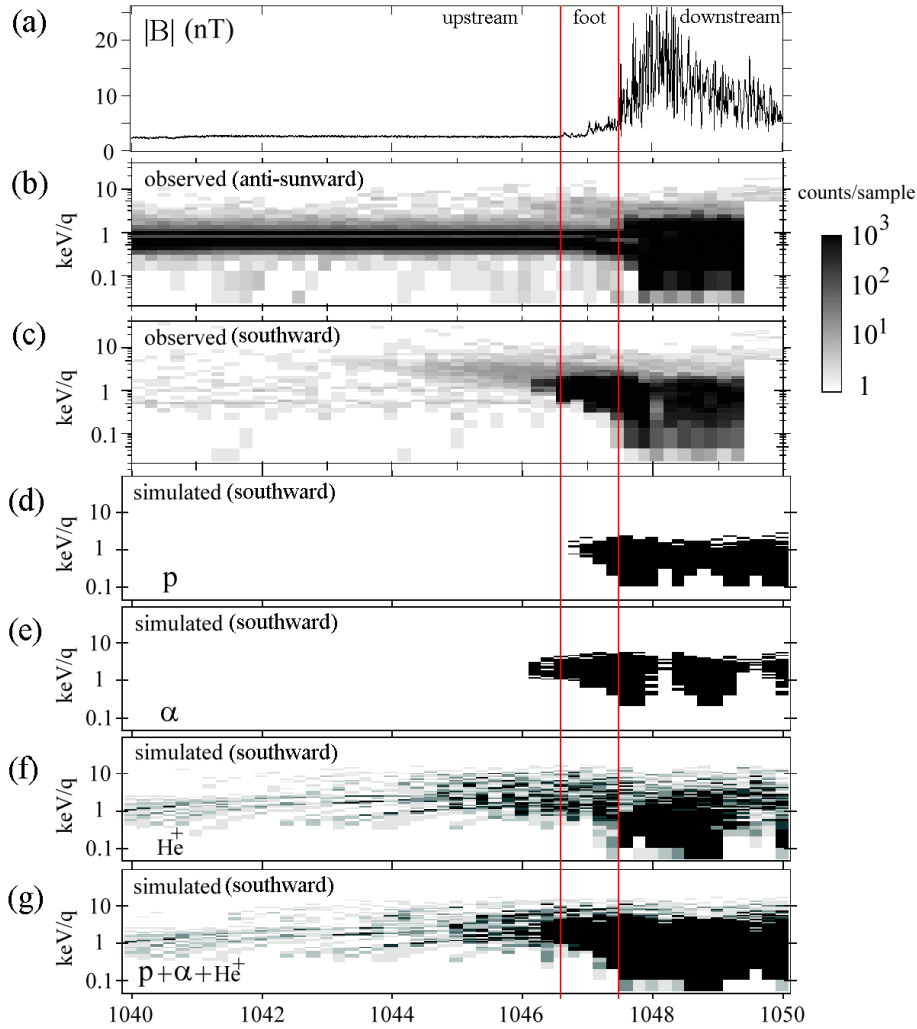


Fig. 2. Data are shown for the period from from 10:40 UT till 10:50 UT on 1 July: (a) magnitude $|B|$ of the magnetic field with 1/16 sec time resolution. (b) Energy-versus-time (E-t) plot for observed ions (0.02-40 keV/q) flowing in the anti-sunward direction. (c) The same as (b) but for ions flowing southward. (d) A simulated E-t plot for southward flowing protons. (e) The same as (c) but for alphas. (f) The same as (d) but for He⁺ ions. (g) The same as (d) but here all species of ions flowing southward are involved (protons, alphas, and He⁺ ions).

Figure 2 (a) shows the magnitude of the magnetic field $|B|$. Thin vertical lines indicate the start (left) and end (right) of the shock foot region. The right edge of the foot region, where the shock ramp is, is due to the identification of the first large spike in $|B|$. On the other hand, the determination of the left side of the shock foot is based on the iterative process using the standard methods to analyze the bow shock (minimum variance, coplanarity, and Rankine-Hugoniot relations) as well as a numerical technique simulating the specular and mirror reflection processes under the prescribed electromagnetic fields (Oka, 2001, in preparation; see Figure 2 (d)-(g)). We use a modeled magnetic field from the smoothed observed data and add noise components generated by the random number generator. For electrostatic field, we use a modeled electrostatic potential following Lipatov et al. (1998). It is found at the same time that this is a supercritical quasi-perpendicular shock crossing with the shock normal vector $\mathbf{n}_S=(0.85,0.27,0.45)$, the up-

stream shock angle $\theta_{Bn1}=76^\circ$ and the shock velocity (in the observers' frame) =10 km/s.

Figure 2 (b) shows the energy-versus-time (E-t) plot for anti-sunward flowing ions, the main component of which is the solar wind protons appearing as a thick black bar having the central energy ~ 0.5 -1 keV/q. (Since the alpha/p ratio was quite low during this event, the solar wind alphas appeared only as the sparse component in the energy range 1-2 keV/q.) The shock thermalization of the solar wind protons is evident as the broadening in this E-t plot in the righthand (downstream) region after the foot region.

Figure 2 (c) shows the E-t plot for ions flowing in the southward direction. Note that the upstream magnetic field was (1.1, -1.7, 0.12) nT, and the $-V \times B$ electric field in the solar wind pointed southward. Therefore upstream ions appearing in this panel are mostly reflected ions being accelerated by this southward electric field after the specular reflection at the bow shock. To understand what is observed

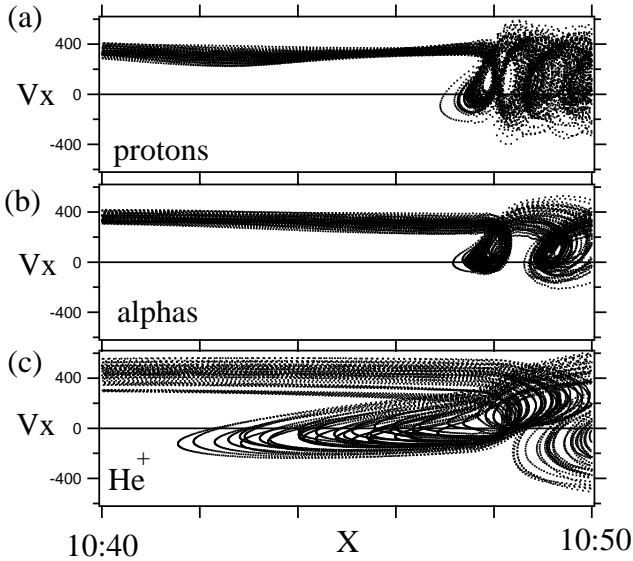


Fig. 3. Examples of orbit tracing are shown projected to the phase space of (X, V_X) : (a) for protons, (b) for alphas, and (c) for pickup He^+ ions. Here the horizontal axis X is represented in terms of time (hour:min) assuming that the shock velocity is 10 km/s so that these plots are directly compared with Figure 2. The unit for V_X is km/s.

in Figure 2 (c) more closely, we have performed test particle simulation, where we inject ensembles of particles (protons and alphas) which are set to have observed velocities and temperatures. Examples of orbit tracing is shown in Figure 3. The relative numbers of ions of different species in the simulation are taken proportional to their observed densities. Figure 2 (d) and (e) are the results of this simulation for protons and alphas, respectively (Here we plot only their reflected components flowing southward). Since the alphas have larger gyroradii, the reflected component reaches further upstream than protons. Comparing these results with the observation in Figure 2 (c), we see that the reflected ions with the darkest gray color consist of protons and alphas. However ahead of the foot region as early as $\sim 10:44$ UT there is a sparse component of the reflected ions (~ 5 keV/q), which had the count rate below 1/100 of the protons. Note also that there are some speckled ions of lower energy ($< \sim 2$ keV/q) extending to $\sim 10:40$ UT in Figure 2 (c). To understand these sparse and speckled components we first attempted to inject various heavy ion component usually found in the solar wind, but could not reproduce the observed E-t plots.

It is noted that in the classical work on the structure of the shock foot region Sckopke et al. (1983) already noted the cases where sparse reflected ions appeared beyond the spatial limit of specularly reflected ions. While these authors suggested the possibility that the non-specular reflection can increase the reach of the reflected ions if the electric field direction is favorable. In the present case, however, the electric field direction is unfavorable so that the non-specular reflection does not contribute to increase the reach of the ions.

We finally came up to the idea to consider the interaction

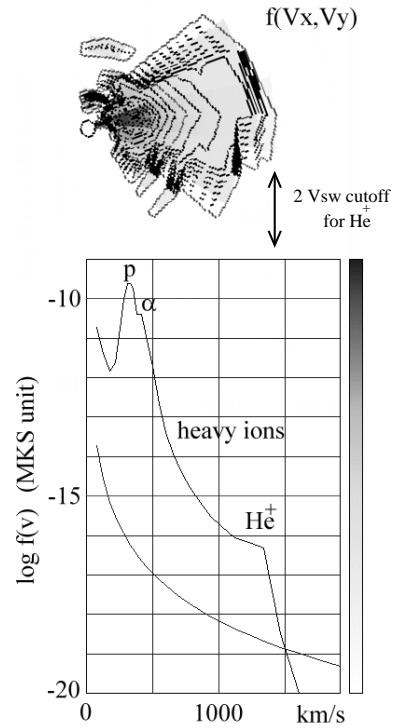


Fig. 4. Observed phase space density $f(\mathbf{V})$ of ions, where a long time accumulation (for ~ 5 hours from 05:02 till 10:14 UT on 1 July 1996, when the solar wind flow was steady) was taken to detect the low density He^+ . Identification of pickup He^+ of interstellar origin is due to the cutoff at $2V_{sw}$. (Since the velocity scale is drawn as if all ions are protons, it should be multiplied by $(M/Q)^{-1/2}$ for ions of mass M and charge Q . Similarly, the phase space density (unit: $\text{m}^{-6} \text{sec}^3$) should be multiplied by $(M/Q)^2$. (Upper) A contour presentation of $f(\mathbf{V})$. (Lower) 1 D cut along the $-V_X$ direction.

of pickup He^+ ions of interstellar origin with the bow shock. Although it has been known that LEP instrument on GEOTAIL is sensitive to pickup He^+ ions (Noda, 2001), there has been no systematic search for their interaction with the bow shock. It is noted that the density of neutral interstellar helium particles at 1 AU and the density of pickup He^+ ions become highest within the gravitational focusing cone, which the earth traverses in early December every year. Although the date of our observation, 1 July, is well outside of the cone, the expected density of pickup He^+ ions is $\sim 1/7$ of its highest value and thus detectable. We have integrated the LEP ion data for several hours and confirmed the existence of He^+ ions (Figure 4). As first discussed by Vasylunas and Siscoe (1976) these pickup He^+ ions make a spherical distribution of the radius of V_{sw} (the solar wind velocity) with its center moving with the solar wind flow. We then injected this distribution of pickup He^+ ions into the bow shock, and trace their behavior. The result is shown in Figure 2 (f) and Figure 3 (c): Mirror-reflected pickup He^+ ions can reach much further upstream than reflected protons and alphas and become a sparse component ($> \sim 5$ keV/q). We have also found a

simple explanation of the speckled component in Figure 2 (c): Since the pickup He^+ ions have broader pitch angle coverage than ions of the solar wind proper, some of them are detected flowing southward during the corresponding gyration phase. Low energy He^+ ions ($< \sim 2$ keV/q) appearing from 10:40 in Figure 2 (f) are actually ions right after their injection.

We then summed up all simulated ion species, protons, alphas, and pickup He^+ ions, and obtained the plot shown in Figure 2 (g). By comparing it with the observation in Figure 2 (c) it is seen that the observed feature is well explained by this model.

3 Remarks

In this paper we present the first identification of the initial acceleration process of pickup He^+ of interstellar origin at the terrestrial bow shock. It is hoped that further event studies of the Earth's bow shock will provide useful database to get more thorough understanding on the physical processes for the interaction of pickup interstellar ions with the solar wind.

Acknowledgements. We thank the team members of the GEOTAIL particle and field measurement for their collaboration.

References

- Ellison, D. C., ApJ 512, 403, 1999.
 Frañz, M., et al., GRL 26, 17, 1999.
 Giacalone, J., and J. R. Jokipii, Space Sci. Rev. 72, 441, 1995.
 Gloeckler, G., et al., Science 261, 70, 1993.
 Gloeckler, G., et al., JGR 99, 17637, 1994.
 Kokubun, S., et al., J. Geomag. Geoelectr. 46, 7, 1994.
 Lee, M. A., V. D. Shapiro, and R. Z. Sagdeev, JGR 101, 4777, 1996.
 Liewer, P. C., and B. E. Goldstein, and N. Omid, JGR 98, 15211, 1993.
 Lipatov, A. S., G. P. Zank, and H. L. Pauls, JGR 103, 29679, 1998.
 Lipatov, A. S., and G. P. Zank, PRL 82, 3609, 1999.
 Mason, G. M., et al., Report of Working Group 6, Space Sci. Rev., 89(1/2), 327, 1999.
 Mobius, E., et al., Space Sci. Rev., 78, 375, 1996.
 Mukai, T., et al., J. Geomag. Geoelectr. 46, 669, 1994.
 Noda, K., Doctorial Thesis, The Univ. of Tokyo., 2000.
 Scholer, M., and H. Kucharek, GRL 26, 29, 1999.
 Schopke, N., et al., JGR 88, 6121, 1983.
 Vasyliunas, V. M., and G. L. Siscoe, JGR 81, 1247, 1976.
 Zank, G. P., et al., JGR 101, 457, 1996.